Computers and Electronics in Agriculture 196 (2022) 106860

Contents lists available at ScienceDirect

Computers and Electronics in Agriculture

journal homepage: www.elsevier.com/locate/compag

Exploiting plant dynamics in robotic fruit localization☆

Jordy Senden [a,*], Lars Janssen [a], Robbert van der Kruk [a], Herman Bruyninckx [a,b], René van de Molengraft [a]

[a] Department of Mechanical Engineering, TU Eindhoven, the Netherlands
[b] Department of Mechanical Engineering, KU Leuven, Belgium

ARTICLE INFO

Keywords:
Autonomous harvesting
Dynamic detection
Frequency response
Fruit localization
System identification

ABSTRACT

The task of harvesting a tomato truss requires the truss to be separated from the stem by severing the peduncle. Challenges to perform this task with an autonomous robotic system include ripeness detection of the truss and localizing the peduncle, which is often done using only a vision system. Occlusion by leaves, stems and other trusses generally hamper vision-based detection. This study proposes a supplementary method to reach the peduncles, based on vibration feedback. This is done by mechanically exciting the tree at the stem and measuring the frequency response. At a certain frequency, the truss will resonate to the excitation. When traveling along the stem, while exciting it, the shift of this resonance frequency indicates the progress towards the peduncle. It is demonstrated that the resonance frequency increases when the distance to the peduncle decreases, which is attributed to a change of the mechanical stiffness of the stem part between the location of excitation and the location of the peduncle. The method is first tested by exciting a mock-up tomato plant with a 1 degree-of-freedom (DOF) actuator and measuring the response. This mock-up behaves like a fourth order mass spring damper system, where the stiffness of one of the modeled springs increases when the distance to the peduncle decreases. Next, the method is tested on a real tomato plant with multiple trusses. It is shown how these trusses contribute to the multiple distinguishable resonance frequencies. The individual contribution of the trusses to the response can be identified due to the superposition principle for linear dynamics. The closest truss has the highest resonance frequency of $3-4Hz$. Similar to the mock-up plant, it is shown that these frequencies increase when approaching the peduncle, with approximately $0.7Hz/m$. The change of the frequencies should be used to track the progress towards a truss, rather than predicting an exact location. This approach is independent of the exact parameters of the plant, resulting in a promising proof-of-concept as extra sensor modality.

1. Introduction

Due to labor shortages in the agro-food industry, there is a need for autonomous systems to help with repetitive tasks, e.g. harvesting tomato trusses and pruning the leaves on tomato trees, grown in greenhouses. For these tasks it is important to be able to detect objects such as tomato trusses, leaves, stems and peduncles. The main difficulty of operating in a natural environment are variations that the systems need to be able to deal with. The objects of interest are never exactly the same, e.g. some tomatoes are bigger than others and not all tomato trusses hold the same amount of tomatoes. An autonomous systems needs to deal with these variations in the product. Another challenge in a natural and dense environment are occlusions. Detecting fruits with a camera is difficult when the fruit is surrounded by dense foliage and other fruits, an example of which is shown in Fig. 1.

The human harvester deals with occlusions in several ways; 1) use prior knowledge to predict where to expect plant parts and 2) use multiple complementary sensor modalities to acquire the necessary data, e.g. when an object cannot be seen it might be felt and vice versa. For example, a peduncle can be occluded but we know it will be located near the top part of the truss. Feeling on top of the truss might result in finding the peduncle, such that we can grab and cut it. The goal is to provide a robot with multiple ways to solve a task in order to deal with variations and occlusions, thus increasing robustness. This includes the use of multiple sensor modalities to retrieve a desired piece of information. The objective of this work is to show a novel truss detection modality, based on vibration feedback.

In Appendix A a list of known harvesting systems is given. The

☆ This project is supported by NWO/TTW.
* Corresponding author.
E-mail address: j.p.f.senden@tue.nl (J. Senden).

https://doi.org/10.1016/j.compag.2022.106860
Received 2 July 2021; Received in revised form 26 February 2022; Accepted 7 March 2022
0168-1699/© 2022 The Authors. Published by Elsevier B.V. This is an open access article under the CC BY license (http://creativecommons.org/licenses/by/4.0/).



Fig. 1. Example of tomato trusses being occluded by multiple stems.

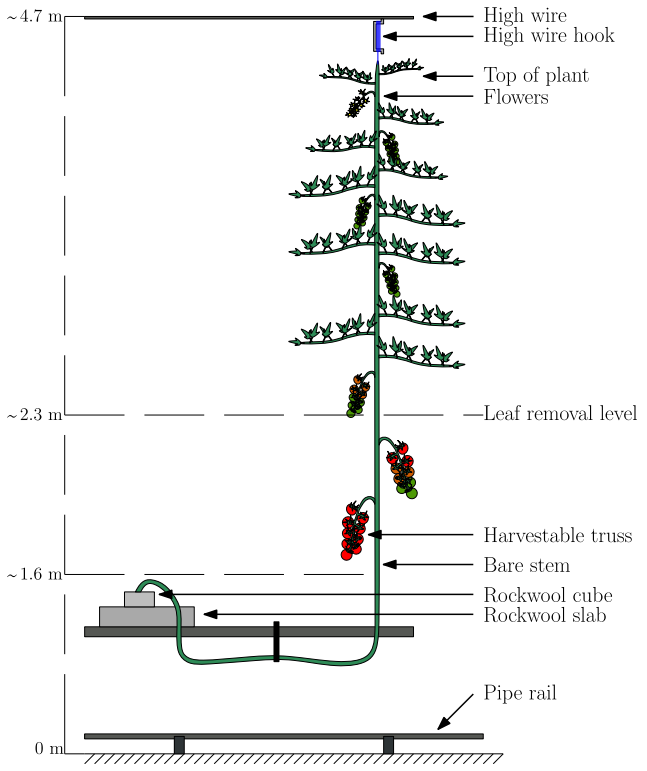

Fig. 2. Schematic overview of a high-wire cultivation system, commonly used to grow tomatoes in the Netherlands. Image based on Hamers (2015) and edited according to Vereijken's greenhouse specifications.

common denominator of these systems is that they rely only on contactless techniques to detect the object of interest. Typically, vision based sensors are used to perform the detection, most common are RGB- or depth cameras. Most research also focuses on vision based detection. Kapach et al. (2012) gives a good overview on classical machine vision techniques using stationary vision sensors, such as single- and stereo RBG camera, RGB-D sensors and spectral- and hyper spectral sensors. Zhao et al. (2016) extends this with thermal imaging sensors and gives an overview of techniques that make use of a moving sensor. More recent detection algorithms use neural network approaches. Koirala et al. (2019) shows how these techniques have been applied for fruit detection and yield estimation.

Next to vision, there are less common approaches for fruit detection. The review in Zujevs et al. (2015) shows that tactile sensors, proximity sensors and chemical sensors (artificial tongue and nose) could be used. Baietto and Wilson (2015) gives an overview of research where an electronic-nose is used to identify fruits and to assess ripeness and quality. These approaches are mainly used for measuring fruit properties or for added safety, shown in Li et al. (2011) and Lehnert et al. (2017).

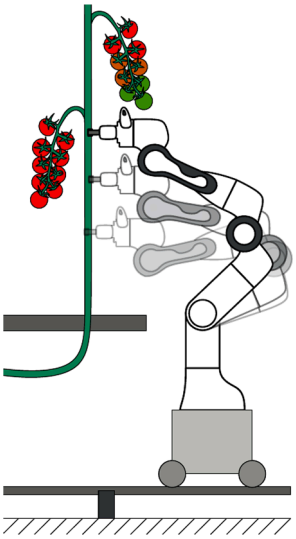

Fig. 3. Visualization of the main-stem-paradigm; a robotic arm on a platform follows the stem until it reaches the peduncle.

Recent research shows how the firmness of apples can be estimated by measuring the frequency response to an excitation Hiruta et al. (2021). In Ding et al. (2021) an overview is given on how acoustic vibrations can be used to determine the quality of fruit. The input signals in these researches are small in amplitude and high in frequency, due to the stiffness of the fruits. Moreover, they are mainly used to detect fruit quality after harvest, not for localization. Localization based on tactile sensors is discussed in Eizentals (2016) and Soetens (2015), where touch sensors are used to detect a stem or peduncle for harvesting. These methods rely on a boolean state of contact; a peduncle or stem is found when contact is made with it. This work aims to extend these tactile truss localization approaches; to identify trusses and estimate the progression made towards them while traveling up the stem, before contact is made. This is done by using dynamic models of how a tomato plant reacts to an excitation. In De Langre (2019) a review is given on how plant dynamics on various scales, e.g. bending of the stem, branch, leaf, fruit or canopy, can be modeled. This dynamic information is mostly used to get an indication of the health of plants. The models discussed in De Langre (2019) include cantilever beam mechanics for bending of plant parts and linear mass spring damper models for plant vibrations. This work extends the use of these models to estimate the distance to a peduncle, by exciting the plant at the stem.

Tomatoes in greenhouses are often of an indeterminate variety, i.e. their growth is not limited. Using a high-wire training system, the plant is kept upright by a twine that hangs on the high-wire via a high-wire hook, schematically shown in Fig. 2. This prevents the plant from succumbing to its own weight. Moreover, this system is useful for flower pollination, light interception on the leaves and plant reachability, increasing labor efficiency (Hamers, 2015). The leaves at the bottom of the plant are removed up to a height of approximately 2.3 meters. This is done to increase air circulation and light penetration, and to provides better access to the tomato trusses for harvesting. Consequently, the bottom part of the plant consists of a free stem with trusses. The ripe trusses that can be harvested hang at a height of approximately 1.6 meters.

When harvesting, the truss needs to be separated from the stem by severing the peduncle. All trusses and leaves are connected, with peduncles and petioles respectively, to the stem of the plant. Thus, following the stem will eventually lead to finding a side branch with either a truss or leaves. This is called the main-stem-paradigm in Soetens (2015). To utilize this approach, schematically visualized in Fig. 3, the system should be able to make contact with the stem and travel along it. The stem can be used as 'the path' to be followed. Following the stem

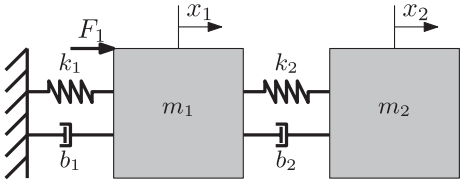

Fig. 4. Schematic representation of a fourth order mass-spring-damper system, with two sets of masses m_i, springs k_i and dampers b_i, where $i = 1, 2$. Both masses move in x_i as a result the applied force F_1.

should be done based on visual- or tactile feedback from sensors in the end effector. The robot arm can move the end effector upwards, while keeping the stem inside the end effector, until a side branch is reached. A high travel velocity is necessary to have a fast localization of a truss. However, the system needs to stop in time before it hits the peduncle to not cause damage to it or the plant. Therefore, an indication of the position of the peduncle, relative to the stem-traveling system, is necessary in order to know when to decrease the travel speed.

From preliminary experiments in Soetens (2015) it is shown that a human can still harvest trusses while being blindfolded. Using tactile information a human can make contact with objects and observe properties like surface roughness and shapes. Next to this, the dynamic response of the environment during interaction gives an indication of properties like mass and stiffness. By shaking and feeling the plant lightly we get a clear feeling of when a truss is shaking heavily, i.e. when we are vibrating a truss in its eigenfrequency. While moving our hands up and down the stem the frequency at which this happens changes. Based on this change we feel whether we are approaching a truss or going further away from it, without knowing the exact distance. This experience is the foundation of the proposed approach. While the system travels along the stem, it can impose a force on the stem and measure its movement, capturing the dynamic response of the plant. The idea is that the presence of the trusses can be detected from the dynamic response due to their relatively high mass. Moreover, it is believed that this response will change depending on the distance between the point of actuation and the location of the tomato truss on the stem. Instead of providing an exact location, the change in dynamic response serves as an indicator on whether the system is progressing to its goal. It tells if the system is approaching the truss or moving farther from it.

First, Section 2 gives background information about the dynamical models that are being used to model the plant. In Section 3 the use of these models is validated by testing on a dummy plant with a single tomato truss. In Section 4 these tests are repeated on a real plant to show how the models can be extended to find multiple trusses. Section 5 explains the significance of the results of this work. Finally, Section 6 presents our findings and discusses future research possibilities.

2. Frequency response of a mass spring damper system

The desired information to retrieve with this detection method is the resonance frequencies of the trusses, not the exact motion of all parts of the plant. When the plant is excited around a fixed equilibrium position, it is assumed that the response can be linearized around this equilibrium point. Therefore, a linear lumped dynamical model existing of masses, springs and dampers can suffice to capture the relevant behavior. In De Langre (2019) it is explained how a second-order linear model can be used to describe the motion of plants at different scales, e.g. the global swaying of a tree, local bending of a branch or the pendular vibration of a fruit. However, this work investigates how the fruit vibrates when the tree is shook, which is a combination of multiple vibration modes. Therefore the second-order model is extended to a higher order.

To describe the movement of a tomato truss with respect to a moving stem, two mass-spring-damper systems are coupled in series. The resulting fourth-order system is shown in Fig. 4 and its transfer function

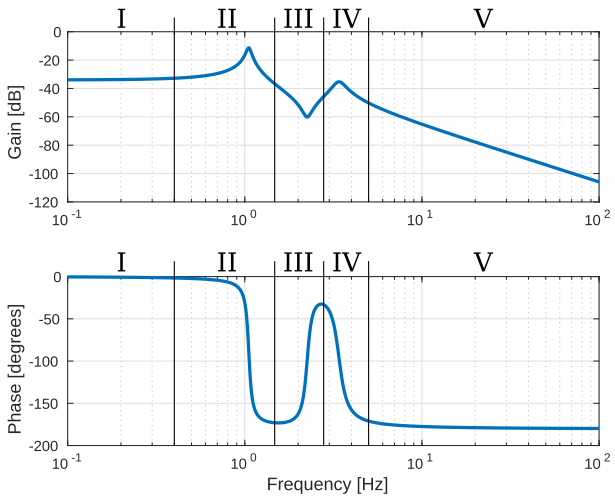

Fig. 5. Bode plot of a fourth order model, with chosen model parameters $m_1 = m_2 = 0.5kg, k_1 = 50Nm, k_2 = 100Nm, \zeta_1 = \zeta_2 = 0.05$. The behavior of the system is split into five regions, as explained in the text.

Table 1
Visual representation of how masses m_1 and m_2, shown in Fig. 4, react to the force F_1 at different sections of the frequency range, shown in Fig. 5. The size and direction of the arrows indicate relative gain and phase delay. A dot indicates no motion.

Section:	F_1	x_1	x_2
I	→	→	→
II	→	→	→
III	→	•	←
IV	→	→	•
V	→	←	•

is calculated as (1).

$$\begin{aligned}
\frac{X_1}{F_1} &= \frac{m_2 s^2 + b_2 s + k_2}{C_4 s^4 + C_3 s^3 + C_2 s^2 + C_1 s + C_0} \\
C_0 &= k_1 k_2 \\
C_1 &= b_1 k_2 + b_2 k_1 \\
C_2 &= b_1 b_2 + k_1 m_2 + k_2 m_1 + k_2 m_2 \\
C_3 &= b_1 m_2 + b_2 m_1 + b_2 m_2 \\
C_4 &= m_1 m_2
\end{aligned} \tag{1}$$

A Bode plot for this system is shown in Fig. 5. The values chosen for this example are: $m_1 = m_2 = 0.5kg, \zeta_1 = \zeta_2 = 0.1, k_1 = 50Nm, k_2 = 100Nm$.

To understand the dynamic behavior of this system, Fig. 5 is split up into 5 regions; I) a low frequency region, II) the first resonance, III) an anti-resonance, IV) the second resonance, and V) the high frequency region. In Table 1 schematic drawings are made to visualize what happens at each of these regions. At the low frequency regions I and II the two masses move in unison to the input force. At the anti-resonance frequency the heavily moving second mass imposes a force on mass one, in anti-phase with the input force. This causes the first mass to barely move. In the regions after the anti-resonance region, the two masses move opposite to each other. This is referred to as dynamic decoupling of the second mass. The resonance peaks in regions II and IV are the frequencies where the denominator of (1) approaches 0, called the poles of the system. For this system there are 4 solutions to let the denominator approach 0; two poles and their complex conjugate. In Fig. 5 a one-sided bode plot is shown, omitting the complex conjugate solution, hence two resonance peaks are visible. The anti-resonance

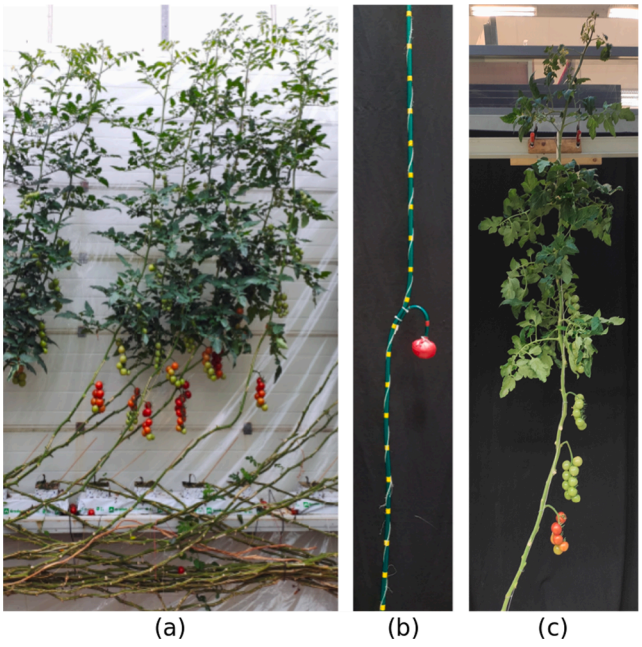

Fig. 6. Pictures of real plants in a greenhouse (a), the dummy plant in the lab (b) and a single real plant in the lab (c).

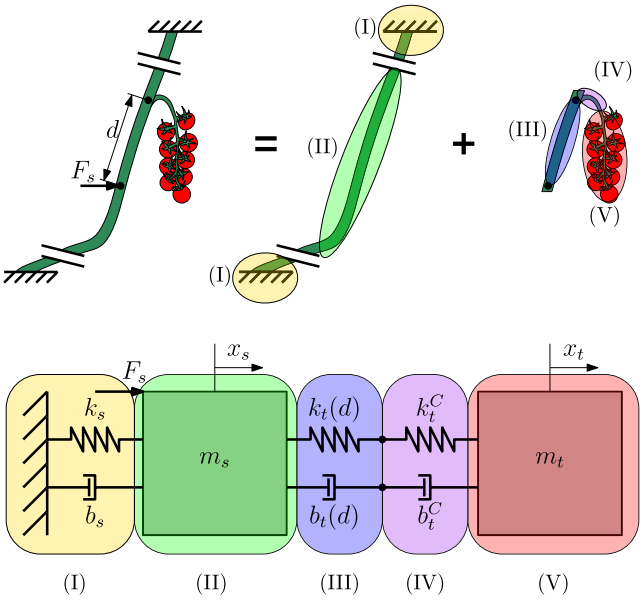

Fig. 7. Schematic representation of the dummy plant, together with the dynamic model. The relevant parts are represented with a number: (I) models the connection of the plant to the fixed world as a spring k_s and damper b_s and (II) represents the mass of the stem m_s. The connection between the truss and stem is modeled as a set of serial springs and dampers. This set consists of a constant part (k_t^C and b_t^C), representing the peduncle (IV), and a part (III) that is dependent on the distance d between the excitation point and the peduncle ($k_t(d)$ and $b_t(d)$). The mass of the tomato truss (V) is modeled as m_t.

peak in region III can be found at the frequency where the numerator of (1) approaches 0, called the zeros of the system.

3. System Identification of a dummy tomato plant

A tomato plant consists of many movable parts, such as the stem, leaves and trusses. Moreover, the environment to which the plant is mounted, e.g. the high wire and plant bed, also introduce dynamics. Manually exciting the trees showed that the resonance frequency of a tomato truss can be felt better than the response from other parts of the plant. This can be explained by the mass of a truss, which is larger than the mass of the leaves. To understand how the model parameters are affected by the plant properties, initial tests are done on a dummy plant with a single tomato truss to ensures a controlled environment. The tests are repeated for a real plant, with multiple tomato trusses.

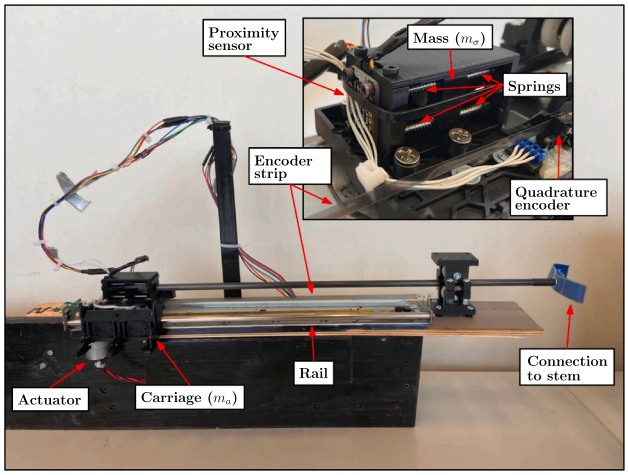

Fig. 8. Picture of the 1DOF setup, with a more detailed view of the carriage and sensors.

3.1. Setup and model of a dummy plant

The dummy plant, shown in Fig. 6, consists of only a stem, one peduncle and one plastic tomato. The fake stem and peduncle are made from a garden hose with an outer diameter of 14*mm*. To give the stem extra mass and stiffness, the garden hose is filled with an XMvK 5*x*1, 5mm^2 cable with an outer diameter of 10*mm*. The plastic tomato is filled with approximately 0.65*kg* of lead to resemble the mass of an entire truss.

A model with two lumped masses is adopted; one representing the movement of the stem and the second representing the movement of the truss w.r.t. the stem. A schematic representation of this model, and how its components reflect the different plant parts, is shown in Fig. 7.

In this model m_s represents the apparent mass of the stem, and everything connected to it, that is felt while pulling the stem from its equilibrium position. The spring k_s makes sure this mass returns to its equilibrium point and the damping d_s attenuates oscillation around this point. Mass m_t represents the mass of the tomato truss, which is attached to the stem with a set of serial springs and dampers. These springs and dampers represent the peduncle (k_t^C and d_t^C) and the part of the stem between the excitation point and the peduncle ($k_t(d)$ and $d_t(d)$). The stiffness and damping constants are linked to the material properties, second moment of inertia of the cross section, and the lengths of the stem and peduncle. Since these properties remain unchanged for the peduncle, while moving along the stem, it is assumed that k_t^C and d_t^C remain constant. However, the distance (d) between the excitation point and the peduncle will change during the movement. This change of length of the part of the stem leads to a changing value of $k_t(d)$ and $d_t(d)$. Due to this change, the apparent stiffness (k_N) and damping (b_N) that is felt also changes, according to (2) and (3).

$$\frac{1}{k_N} = \frac{1}{k_t(d)} + \frac{1}{k_t^C} \tag{2}$$

$$b_N = b_t(d) + b_t^C \tag{3}$$

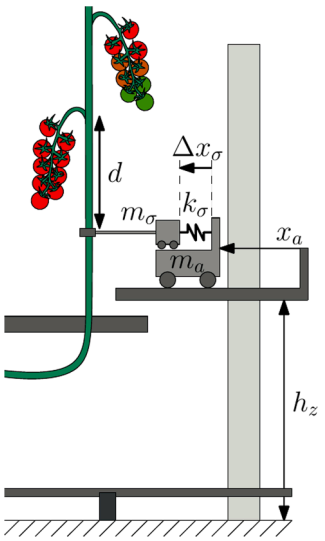

Fig. 9. Schematic overview of the test setup, where the actuator is connected to the stem at a distance d to the peduncle. The position of the actuator on a slide x_a and the displacement Δx_σ of the connection with respect to the actuator are measured. The mass m_σ of the connection is deemed negligible with respect to the mass of the stem and trusses. The applied force to the stem can be estimated with (4), while the displacement of the stem is calculated with (5).

3.2. Excitation- and force-sensing system

To measure the frequency response of the plant, a system is needed that can shake the plant while measuring the excitation position and force. The system needs to be able to connect to the plant at different heights, to test at different distances from the peduncle. Eventually these capabilities should be integrated into the harvesting system, e.g. a robotic arm as shown in Fig. 3. This system should be able to perform both the excitation and the traveling along the stem, preferably simultaneously. For this proof of concept a 1DOF actuator, shown in Fig. 8, was made to perform the excitation and force sensing. Traveling up the stem is emulated by performing sequential measurement, where the 1DOF actuator is manually placed at a different height (h_z). The system is connected to the plant by tightly wrapping a Velcro strap around the stem, emulating the grasp of a robotic end effector. A schematic overview of the test system is shown in Fig. 9.

The picture and overview show a carriage (m_a) that can travel along a sliding rail of approximately 30cm. The position of this mass (x_a) is measured by a HP CB781-80006-A quadrature encoder, in combination with an encoder strip with 40 counts per millimeter. A calibrated proximity sensor (VCNL4040) is mounted on top of the moving mass that measures the distance (x_σ) to the lightweight Velcro strap that is connected to the stem. The small mass of this connection (m_σ) is assumed to be negligible with respect to the mass of the stem and tomatoes. The stiffness of the springs $k_\sigma = 0.72Nm$ is known from the manufacturer and validated through calibration measurements. By measuring the distance x_σ, the force between the stem and the actuator can be estimated with (4). The position of the connection point is calculated with (5). Measuring the displacement x_s as a result of the applied force F_a gives the dynamic response of the plant, as discussed in Section 2.

$$F_a = k_\sigma \Delta x_\sigma \tag{4}$$

$$x_s = x_a + \Delta x_\sigma \tag{5}$$

3.3. Experiments and results on dummy plant

In these experiments, the dummy plant is connected with a trellising wire to the roof, at a height of approximately 3 meter. The low end of the stem is draped on the floor loosely and to the left, resembling tomato plants in a greenhouse. The truss is connected to the stem at a height of 1.5 meter, measured from the floor. The dummy plant for these experiments can be seen in Fig. 6. The plant is excited with the system discussed in Section 3.2 at 8 different positions below the peduncle connection point. To excite the system, a logarithmic sine sweep is used to put more emphasis on the low frequency region. The sweep lasts 5 min per measurement, with increasing frequency between 0.5 and 10Hz. During initial tests it was found that the dynamics of interest resided well within this range. Since the bode-plots are plotted on a logarithmic scale, a logarithmic sine sweep ensures equal time is spent at each frequency on the logarithmic x-axis. The force applied to the plant is measured during this sine sweep. To assess reproducibility, multiple measurements are repeated at each distance. Fig. 10 shows the frequency response of three measurements, performed at a distance of 8cm below the truss. Comparing these results to Fig. 5 shows that the dummy

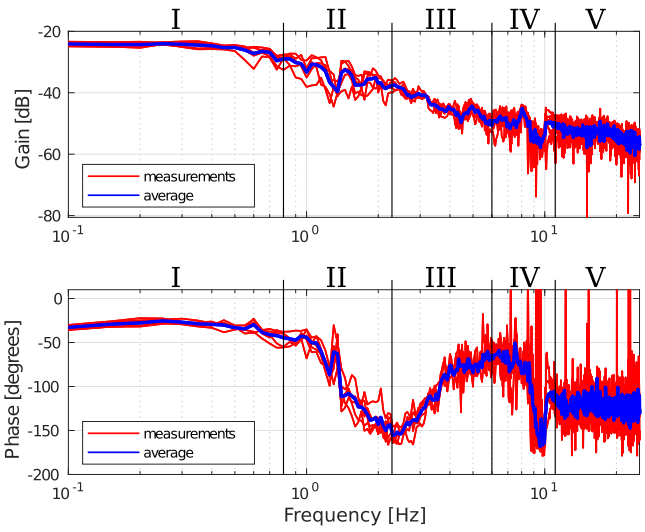

Fig. 10. Bode plots of five repeated measurements on the dummy plant at 8cm below the truss, including the averaged bode plots. The similarities with Fig. 5 indicate that the dummy plant acts as a fourth order system.

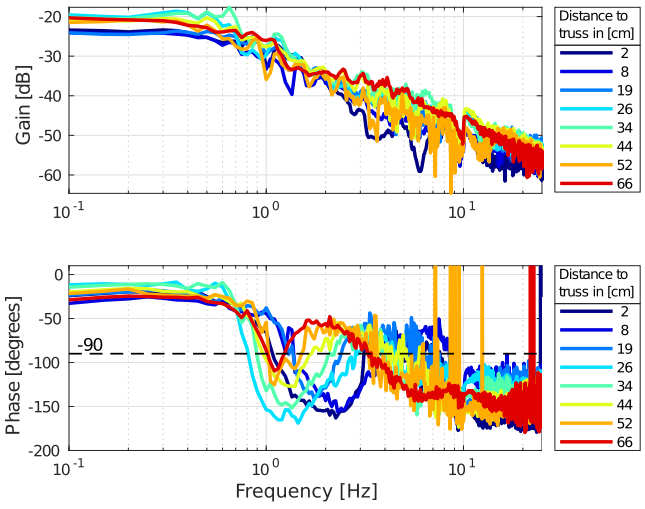

Fig. 11. Frequency response of the dummy plant with a truss, connected at a height of 150cm from the floor. The stem is excited at different distances below the truss, measured in cm. This plot shows the average response of multiple measurements at each given height. It can be seen that the anti-resonance frequency, where the phase crosses the -90 degree line upward, increases when the distance to the peduncle decreases.

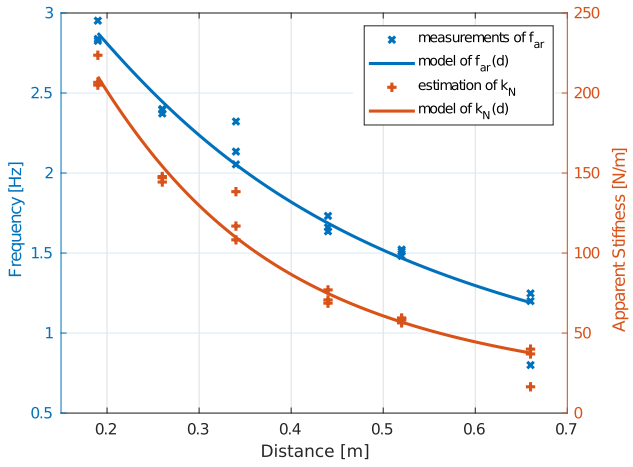

Fig. 12. In blue, the measured anti-resonance frequency as a function of the distance to the peduncle and a fit of (10) with the parameters given in Table 2. In orange, the apparent stiffness k_N as a function of the distance to the peduncle, estimated using (7).

plant acts as a fourth order system. The overlapping lines, for each measurement at this height, show that measuring the frequency response of the system is reproducible.

The resonance frequency in region II, indicated by a significant phase-drop, is caused by the dynamics of the stem. This is the frequency at which only a small force is needed to make the stem and truss move in unison. Between 3 and 4Hz the phase delay of the systems crosses the -90 degrees. This is the anti-resonance frequency, were the truss dynamically decouples from the stem, as explained in Section 2. This anti-resonance frequency is dependent on the mass of the truss and the apparent stiffness between the actuator and the truss. The mass of the truss stays constant, while the apparent stiffness is a function of the distance to the peduncle. Therefore, this anti-resonance frequency can be used as a qualitative indicator for the distance to the peduncle.

This experiment is repeated for different distances to the truss. The results of these measurement are shown in Fig. 11. This figure is created by averaging the measurements at each distance.

In order to understand the dependency of the apparent stiffness (k_N) in relation to the distance between the actuator and peduncle, the anti-resonance frequency (f_{ar}) is determined for all measurements. This is done by finding the frequency at which the phase delay increases and crosses the -90 degree line, shown in Fig. 11. In Fig. 12 this anti-resonance frequency is shown for all measurements at different distances. From this figure it can be clearly seen that the anti-resonance frequency increases when the distance to the peduncle decreases.

The blue line in Fig. 12 represents a model that is fitted to the measured data. This fit is based on the fourth-order model of the plant, where the anti-resonance frequency (f_{ar}) is found when (1) approaches zero. This anti-resonance frequency is calculated as (6) and is linked to the apparent stiffness and mass of the truss.

$$f_{ar} = \frac{1}{2\pi}\sqrt{\frac{k_N}{m_t}} \tag{6}$$

From (2) the apparent stiffness can be calculated as (7).

$$k_N = \frac{k_t^C k_t(d)}{k_t^C + k_t(d)} \tag{7}$$

The stiffness of the part of the stem between the actuator and the peduncle connection point is caused by the way this part of the stem bends De Langre (2019). Following cantilever-beam mechanics Fenner (1998), the relation between the force exerted and the bending of the stem is often of the form as shown in (8). Here, δx is the bending

Table 2
Values found for fitting model (10) to the data, shown in Fig. 12.

Parameter	Value	Unit
m_t	0.65	kg
e	2	-
k_t^C	359.4	Nm^{-1}
α	0.055	$N^{-1}m^{-1}$

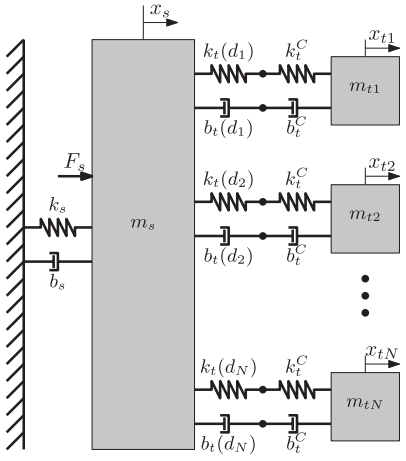

Fig. 13. Schematic representation of a real plant, containing N tomato trusses. Each truss is modeled as a mass-spring-damper pair, leading to a system of order $(N+1)^2$. The apparent spring constant of each truss will be different, since the distance to each truss is different.

displacement of the stem, F is a force exerted on the beam at distance l, e is an integer exponent (often 2 or 3). The parameter α relates to the geometric- and material properties of the stem.

$$\delta x = \alpha l^e F \tag{8}$$

A linear spring, adhering to Hook's law, reacts to a force according to $F = k\delta x$. The springlike force felt by bending a beam can be derived from (8), which results in the spring constant of the beam (k_b) given by (9).

$$k_b = (\alpha l^e)^{-1} \tag{9}$$

Assuming the stiffness of the stem ($k_t(d)$) behaves similarly, combining (9) with (7) will lead to the model shown in (10).

$$f_{ar} = \frac{1}{2\pi}\sqrt{\frac{k_t^C}{m_t(\alpha k_t^C d^e + 1)}} \tag{10}$$

This model is fitted to the data using a least squares method, as shown in Fig. 12. The resulting values for the parameter of the model in (10) are given in Table 2.

Using the measured anti-resonance frequency and the model in (10), the apparent stiffness can be estimated as (11). The result of this estimation is shown in Fig. 12.

$$k_N = \frac{k_t^C}{\alpha k_t^C d^e + 1} \tag{11}$$

4. Experiments on a real tomato plant

The experiments on the dummy plant indicate that a fourth-order mass-spring-damper model suffices to capture the relevant dynamics of a plant with one truss. Real plants however, often have multiple trusses and leaves which can cause a different response. Tests have been done on a real plant to see whether the relation between the resonance frequency and the distance to the truss still holds. Moreover, it is tested whether a distinction can be made between multiple trusses.

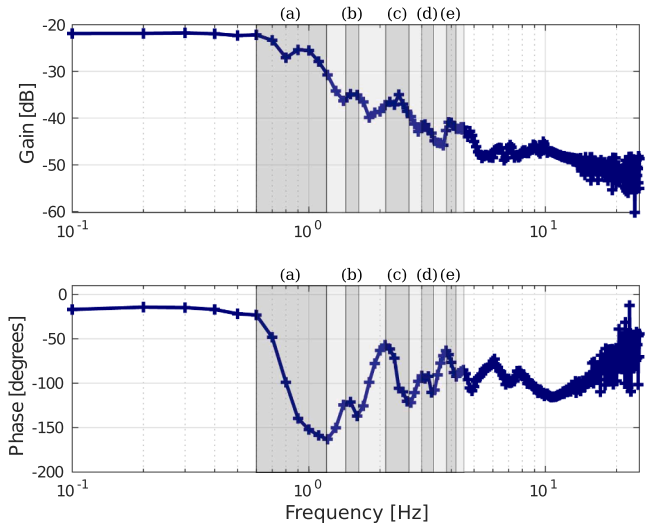

Fig. 14. Bode plot of the average response of multiple measurements where the plant is actuated at $1cm$ from the lowest peduncle. The highlighted frequency ranges (a) to (e) represent frequencies at which a resonance frequency is observed, as visualized in Fig. 15.

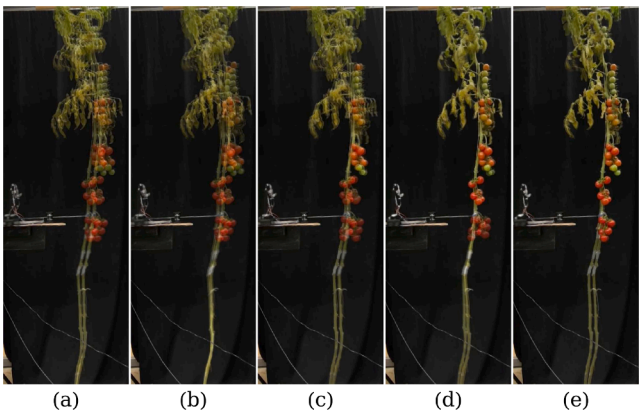

Fig. 15. Five images corresponding to the five frequency ranges in Fig. 14. The images are constructed by overlaying multiple frames in a video, when the plant is moving at its corresponding frequency. Blur indicates movement, while sharpness indicates that the plant part is standing still. In image a) all parts are blurry due to movement, while at e) all tomatoes are hanging still and only the leaves and lower stem part is moving. At even higher frequencies, only the leaves at the top are moving. Between a) and e) a consecutive decoupling of the trusses is observed.

4.1. Model of a real plant

A real live tomato plant is hung up in the lab, as can be seen in Fig. 6. For these tests, a similar approach is taken as discussed in Section 3.3. The model shown in Fig. 7 is extended with multiple masses that represent tomatoes. The schematic overview of the extended model is shown in Fig. 13.

The transfer function between the force F_s and the position of the contact point X_s can be calculated as (12). Here m_s, b_s and k_s represent the mass, spring- and damping constant of the real plant respectively. The masses m_i, spring constants $k_t(d_i)$ and damping constants $b_t(d_i)$, where $i = 1,2,3\ldots N$, represent the N trusses hanging at different heights. Solving (12) for $N = 1$ will result in the fourth order system, derived in (1).

$$\begin{aligned} \frac{X_s}{F_s} &= \left(S_s - \sum_{i=1}^{N} \left(\frac{C_i^2 - C_i S_i}{S_i} \right) \right)^{-1} \\ S_s &= m_s s^2 + b_s s + k_s \\ S_i &= m_i s^2 + b_i s + k_i \\ C_i &= b_i s + k_i \end{aligned} \tag{12}$$

The lowest truss is represented by $i = 1$, while the last felt truss is represented by $i = N$. Using this numbering, a priori knowledge is derived from the tests with the dummy plant and from experience with the real plants. From the results shown in Fig. 12 and given that $d_1 < d_2 < \ldots < d_N$, it is expected that $k_t(d_1) > k_t(d_2) > \ldots > k_t(d_N)$. Moreover, since the weight of a truss increases over time and the oldest trusses hang at the bottom of the plant, it is generally safe to assume that $m_{t1} > m_{t2} > \ldots > m_{tN}$. Without having to know the actual values of these parameters, it will give insight in the resulting bode plots of the frequency response of the real plant. From the transfer function in (12) it can be seen that this system approaches zero each time $S_i = 0$, resulting in an anti-resonance. In other words, each time an eigenfrequency of one of the trusses is reached, this truss will dynamically decouple from the motion of the stem. This is similar to the behavior of the dummy plant with one truss, as explained in Section 3. The eigenfrequency of truss i is calculated as $f_{ni} = \frac{1}{2\pi}\sqrt{\frac{k_i}{m_i}}$.

4.2. Experiments and results on a real plant

The experiments on the real plant are the same as on the dummy plant, as discussed in Section 3.3. A logarithmic sine sweep between $0.5 - 10Hz$ is used to excite the plant while measuring the force applied to the stem and the resulting movement. Fig. 14 shows the average response of multiple measurements where the plant is actuated at $1cm$ from the lowest peduncle.

The highlighted frequency ranges (a) to (e) represent frequencies at which a resonance frequency is observed. The ranges between these regions contain anti-resonance frequencies. Each resonance region represents a mode at which the plant is vibrating. Five of these modes are visually shown in Fig. 15, where each mode corresponds to a frequency region in Fig. 14.

To show the motion of each mode, a video is made during the measurements. An overlay of two frames is made to show where the most motion is happening in the plant. This method of showing motion is comparable to capturing an image with a long shutter time. If the plant part is sharp in the image, this means this part has not moved in between the two frames. If the plant is blurry, this is an indication of movement. Comparing Fig. 14 with Fig. 15 it can be seen that at the lowest resonance range (a) all trusses are moving together with the stem, indicated by a completely blurry plant in the image. At the next range (b), it seems that the masses are decoupled from the movement of the stem, since the stem is in focus while the trusses are blurry. At the following consecutive ranges the trusses decouple one by one, starting with the third truss (c), then the second (d), then the closest (e). If all trusses are decoupled, only the lower part of the stem is still seen moving. At increasingly higher frequencies, only the leaves at the top are moving until nothing moves at all. This would result in a completely clear image of the plant. The clear separation between the resonance ranges indicate this method can be used to distinguish the tomato trusses based on their dynamic response. Similar to the dummy plant, these experiments are repeated in order to see how the response changes at different distances to the peduncle. The average bode plots for multiple measurements at four different heights

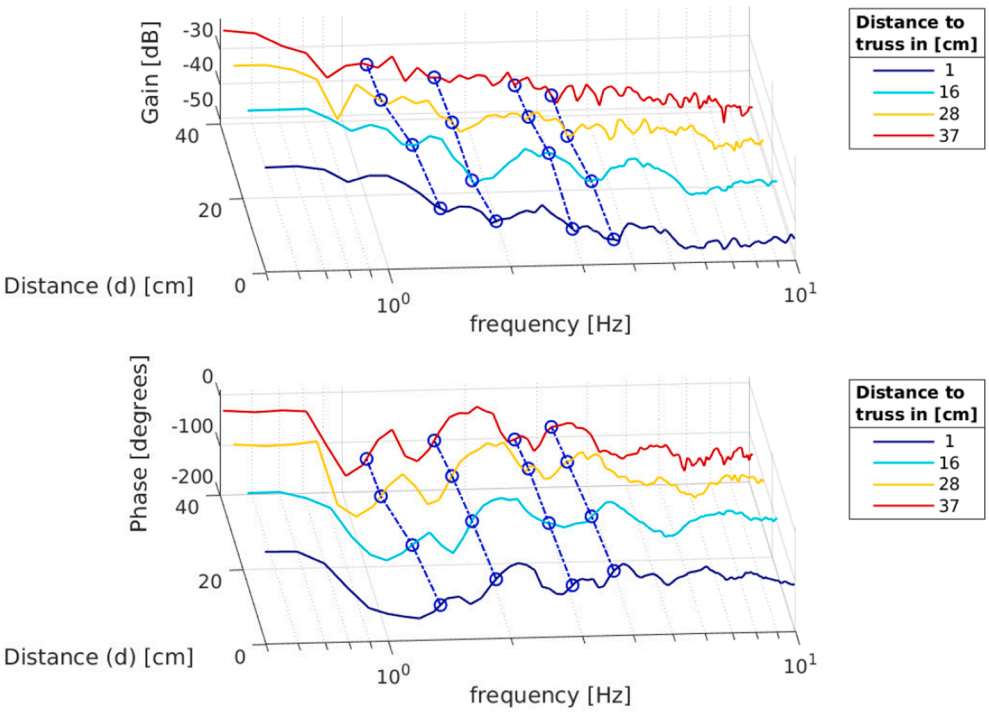

Fig. 16. Frequency response of a real plant with a multiple trusses. The stem is excited at different distances below the truss, measured in *cm*. This plot shows the average response of multiple measurements at each given height. The blue circles indicate the anti-resonance frequencies, indicated by a phase increase, of the four trusses at different distances.

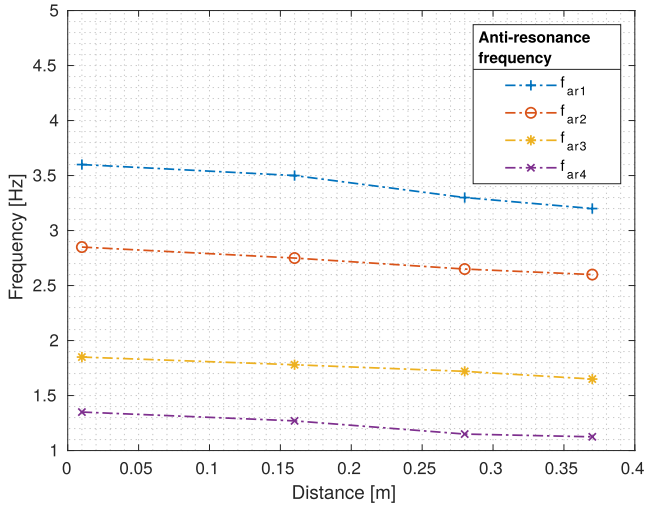

Fig. 17. Anti-resonance frequencies of the four trusses at different distance to the first truss.

are shown in Fig. 16.

This figure shows the bode plot of the response at different distances to the first truss. For each measurement, similar peaks are found as discussed in Fig. 14. For each measurement at different distances the anti-resonance frequencies of the four trusses are indicated with blue circles. In Fig. 17 the anti-resonance frequencies of the four trusses at different distances is shown.

It can be seen that all anti-resonance frequencies increase when the distance to the first peduncle decreases, with approximately $0.7Hz/m$. This is in accordance with the measurements on the dummy plant. A shorter distance to the peduncle results in a higher bending stiffness of the plant. When starting from the bottom, getting closer to the first peduncle necessarily means getting closer to the other trusses as well. This is why all anti-resonance frequencies increase.

5. Discussion

A tomato truss can be located by traveling up the stem of the plant until a peduncle is found. The dynamic response of the plant to an excitation force can be used track the progression towards the truss. This relative truss localization method is complementary to vision based fruit localization techniques. Using a dummy plant with a single truss, it is shown that an anti-resonance frequency is felt when the motion of the truss decouples from the stem. The tests on both the dummy plant and the real plant show that this frequency will become higher when the distance to the truss becomes shorter. The anti-resonance frequencies felt on the real plant happen at the eigen-frequencies of each truss. These frequencies are distinguishable for the first three trusses, where the truss with the highest eigen-frequency is closest to the actuator. Approaching the trusses cause the eigen-frequencies of all trusses to increase. This method works without the need of exact values for the masses, springs and dampers in the model. Instead of identifying the exact parameters in the model, the resonance frequencies need to be determined at different actuation positions. Tracking if these frequencies increase or decrease give enough information to know whether we are approaching a tomato or moving farther from it.

It should be considered that the tests in this work are done on a single

tomato plant. The test plants were hanging free to avoid issues caused by surrounding plants. In a real greenhouse crossing and hooking stems will affect the measurement. This could act as occlusions in the force domain, resulting in the inability to 'feel' the trusses. Secondly, the effect of the orientation of trusses on a stem is not investigated. It is highly likely that this orientation with respect to the actuation direction has an effect on the measurement. There might be a slight shift in resonance frequency or amplitude when a truss is not hanging perpendicular to the direction of motion of the actuator. Another future challenge is to incorporate this proposed sensor modality with a vision-based detection algorithms.

6. Conclusions

We have shown a proof-of-concept on how the dynamic response of a tomato plant could be used to find tomato trusses. Since it is now known at which frequency ranges the trusses start resonating, a system can be designed to measure and actuate at these specific frequencies. The proposed solution would be a add-on system that can be attached to a robot arm, such as illustrated in Fig. 3. Moreover, instead of searching for anti-resonances while sweeping over a range of frequencies, faster detection methods can be investigated. Since the closest tomato will give the highest resonance frequency, all low-frequency excitation could be omitted. As soon as a resonance frequency is found at one position on the stem, the shift in this frequency can be tracked while continuously moving along the stem. A possibly faster approach would be to use a time based detection strategy.

CRediT authorship contribution statement

Jordy Senden: Conceptualization, Methodology, Software, Investigation, Writing – original draft. **Lars Janssen:** Software, Investigation, Writing – original draft. **Robbert van der Kruk:** Writing – review & editing. **Herman Bruyninckx:** Writing – review & editing, Supervision. **René van de Molengraft:** Conceptualization, Writing – review & editing, Supervision.

Declaration of Competing Interest

The authors declare the following financial interests/personal relationships which may be considered as potential competing interests: [Jordy Senden reports financial support was provided by Netherlands Foundation of Scientific Research Institutes.]

Acknowledgment

This project is supported by NWO/TTW. The authors would like to thank Vereijken Kwekerijen for providing us with real tomato plants.

Appendix A. Existing harvesting systems

The process of harvesting tomato trusses is similar to harvesting other fruits, such as cucumbers, sweet peppers, strawberries and many more. The techniques developed for one fruit could be used on another. Depending on the country in which research is performed, or companies are started, the focus might be on a different fruit. In Bac et al. (2014) and Bachche (2015) an overview is given of research done in the field of fruit harvesting robots from 1984 until 2014. The amount of research in this field has only increased since then and resulted in a number of working systems and prototypes. In Table 3 a list of existing autonomous harvesting and pruning systems is shown.

Table 3
Known fruit harvesting and leaf pruning systems.

Harvesting		
Project (year)	*Region*	*Fruit*
Agribot (2011)	Suzhou City, Jiangsu, China	Tomato
Agrobot (2018)	La Palma del Condado, Huelva, Spain	Strawberry
Agronauta (2015)	Almeria, Spain	Tomato
Berry 5 (2015)	Tampa, Florida, USA	Strawberry
CATCH (2016)	Garching bei Munchen, Germany	Cucumber
Crux Agribotics (2015)	Eindhoven, Netherlands	Cucumber
Dogtooth (2014)	Royston, England	Strawberry
Fieldwork Robotics Ltd. (2017)	Plymouth, England	Raspberry
GIGAS (2017)	Guelph, Ontario, Canada	Tomato
GRoW (2018)	Migdal HaEmek, Israel	Tomato
Inaho (2017)	Kanagawa, Japan	Tomato
Root.AI (2018)	Somerville, Massachusetts, USA	Tomato
Rubion (2009)	Leuven, Belgium	Strawberry
Panasonic (2018)	Osaka, Japan	Tomato
Sweeper (2015)	Wageningen, Netherlands	Sweet Pepper
Uni of Essex (2018)	Essex, England	Strawberry
Pruning		
Project	*Region*	*Fruit*
Bloom Automation (2016)	Woburn, Massachusetts, USA	Cannabis
Grapevine Pruner (2009)	San Diego, California, USA	Grape
Priva Compano (2016)	De Lier, Netherlands	Tomato
TrimBot2020 (2016)	Wageningen, Netherlands	(bush) Grape
Vine Pruner (2016)	New Zealand	Grape

References

Bac, W.C., Henten, E.J.V., Hemming, J., Edan, Y., 2014. Harvesting Robots for High-value Crops: State-of-the-art Review and Challenges Ahead. J. Field Robot. 31 (6), 1–24.
Bachche, S., 2015. Deliberation on Design Strategies of Automatic Harvesting Systems: A Survey. Robotics 4 (2), 194–222.
Baietto, M., Wilson, A., 2015. Electronic-nose applications for fruit identification, ripeness and quality grading. Sensors (Basel, Switzerland) 15, 899–931.
De Langre, E., 2019. Plant vibrations at all scales: A review. J. Exp. Bot. 70 (14), 3521–3531.
Ding, C., Feng, Z., Wang, D., Cui, D., Li, W., 2021. Acoustic vibration technology: Toward a promising fruit quality detection method. Comprehensive Rev. Food Sci. Food Saf. 20 (2), 1655–1680.
Eizentals, P., 2016. Picking System for Automatic Harvesting of Sweet Pepper. PhD thesis, Kochi University of Technology.
Fenner, R.T., 1998. Mechanics of solids. Blackwell Scientific Publications.
Hamers, A., 2015. Designs for mechanization of greenhouse truss tomato crop maintenance. Master thesis, TU/e.
Hiruta, T., Hosoya, N., Maeda, S., Kajiwara, I., 2021. Experimental evaluation of frequency response and firmness of apples based on an excitation technique using a dielectric elastomer actuator. Sensors Actuators A: Phys. 330, 112830.
Kapach, K., Barnea, E., Mairon, R., Edan, Y., Ben-shahar, O., 2012. Computer vision for fruit harvesting robots– state of the art and challenges ahead. Int. J. Comput. Vision Robot. 3 (1/2), 4–34.
Koirala, A., Walsh, K.B., Wang, Z., Mccarthy, C., 2019. Deep learning–Method overview and review of use for fruit detection and yield estimation. Comput. Electron. Agric. 162 (April), 219–234.
Lehnert, C., English, A., Mccool, C., Tow, A.W., Perez, T., 2017. Autonomous Sweet Pepper Harvesting for Protected Cropping Systems. IEEE Robot. Automat. Lett. 1–8.
Li, Z., Li, P., Liu, J., 2011. Physical and mechanical properties of tomato fruits as related to robot's harvesting. J. Food Eng. 103 (2), 170–178.
Soetens, R., 2015. Towards Automatic Harvesting of Truss Tomato in a High-Wire Cultivation System. Master thesis, TU/e.
Zhao, Y., Gong, L., Huang, Y., Liu, C., 2016. A review of key techniques of vision-based control for harvesting robot. Comput. Electron. Agric. 127 (September 2016), 311–323.
Zujevs, A., Osadcuks, V., Ahrendt, P., 2015. Trends in Robotic Sensor Technologies for Fruit Harvesting: 2010–2015. Procedia Comput. Sci. 77, 227–233.